Curr. Pharm. Res. **2019**, *419,* 154-163

Current Pharma Research
ISSN-2230-7842
CODEN-CPRUE6
www.jcpronline.in/

Research Article

Theme- *New horizons in chemical sciences.*
Guest Editor- *R.P. Pawar*

Visible-light Photocatalytic activity of Cr-doped TiO_2 nanoparticles by modified sol-gel method.

Dinkar V. Aware*, Nitin D. Bhoge

M.E.S. Department of Chemistry, Shri Dnyaneshwar Mahavidyalaya, Newasa, Maharashtra, India.

Received 16 March 2019; received in revised form 12 September 2019; accepted 13 October 2019

***Corresponding author E-mail address:** *awaredinkar@gmail.com*

ABSTRACT
Chromium doped Titania nanoparticles have been successfully synthesized by the modified sol-gel process. After calcinations at 500^{o}C, the resultants nanomaterials have been characterized by XRD, SEM-EDX, TEM-HRTEM, and UV-vis absorption spectroscopy. The powder XRD result revealed that a decrease in grain size with an increase in dopant concentration. The SEM micrographs revealed the spherical-like irregular morphology while EDX confirms the presence of a proper proportion of elements. The absorption edges of TiO_2 nanoparticles shift towards longer wavelengths (i.e. red-shifted) from 400 nm to 700 nm with increasing Cr concentration, which greatly enhances TiO_2 nano-materials on the absorption of the visible light spectrum. The small grain size, high crystallinity, and decrease in the bandgap energy of doped Titania may be responsible for the high photocatalytic activity.

KEYWORDS
Cr-doped TiO_2, Sol-Gel, XRD, SEM; EDX; UV-Vis DRS, dye degradation.

1. INTRODUCTION

In recent times, heterogeneous photocatalysis is widely applied to control environmental pollution[1-5]. The semiconducting materials such as TiO_2, ZnO, WO_3, SnO_2, CuO, Cu_2O, NiO, $BaTiO_3$ play a most important role for complete oxidation and removal of toxic organic waste including various types of textile dye and hazardous organic waste from aqueous phase [6-11]. Among the various semiconducting materials, the titania-based system has received much attention because of its high efficiency and reactivity, good chemical stability, non-toxicity and low cost [12]. However, its environmental applications in real life are still limited due to its wide bandgap energy of anatase titania (3.2 eV) and high electron-hole pair (e^-/h^+) recombination rate [9, 10, 13, 14]. Hence, photocatalytic applications of titania are limited to only 5% solar light radiations (UV light). The tremendous efforts have been carried out to develop titania-based photocatalyst that can work under visible light[15, 16] including surface modification [17-19], doping with metals [20-22] and nonmetals [23-28]. Moreover, doping with the transition metal ions such as Fe^{3+}, Cr^{3+}, V^{5+}, Mo^{6+}, Ni^{2+} Cu^{2+}, Zn^{2+}[6**, 7,** 29-34] has been reported to be an effective method to enhance the photocatalytic activity of titania. Among the various transition metal ions, Cr^{3+} is considered to be an ideal candidate due to its suitable radius and energy level. Both Cr^{3+} (0.755 nm) and Ti^{4+} (0.745 nm) have nearly the same ionic redia and hence [20, 21], Cr^{3+} ions can be easily incorporated into the lattice of TiO_2. The doping of chromium in titania lattice shifts the absorption spectra towards the visible region and enhance its photocatalytic activity [22].

However, some reports showed that chromium doping results from the decrease in the photocatalytic activity of titania due to the creation of additional oxygen vacancies which acts as a recombination center for e^-/h^+ pairs [23]. Various factors like particle size, crystalline phase affect the photocatalytic activity of chromium doped titania [24].

To understand controversies in the results, the present work deals with the synthesis of chromium doped titania nanoparticles by the modified sol-gel method. The resultant nanomaterials were successfully tested for photodegradation of methyl red as a model pollutant.

The Introduction must contain an accurate and concise analysis of the existing knowledge of the investigated scientific problem. A very broad overview of the scientific topic and related background, as well as the compilation of a long list of cited references, should be avoided. The most illustrative citations should be included using the Author-Year citation style. The final paragraph should indicate the motivation and objectives of the conducted work.

2. MATERIALS AND METHODS

2.1. Experimental

Mesoporous Cr (III) doped TiO_2 nanoparticles were synthesized by the surfactant template-assisted sol-gel method. The dopant Chromium (III) nitrate nonahydrate [$Cr(NO_3)_3$ 9H2O] was obtained from SD Fine Chemicals ltd while Titanium (IV) butoxide [$Ti(C_4H_9O)_4$], was obtained from Sigma-Aldrich (USA). Drumstick gum was used as a surface directing agent while Isopropanol, ethanol and deionized water were used as solvent throughout the reaction.

2.2. Synthesis of photocatalyst by modified sol-gel method.

The synthesis of Titania (TiO_2) nanoparticles was carried out by a modified sol-gel method using a water-alcohol mixture as a solvent. In a typical synthetic process, a solution containing 160 ml of ethanol and 20 ml of isopropyl alcohol were mixed slowly with 20 grams of Titanium (IV) butoxide under sonication at 40°C in the ultrasonic bath for 30 minutes for proper dispersion. To this, 2 grams of alcoholic gum powder was added drop by drop with constant magnetic stirring. The resultant precursor solution was mixed with 100 ml distilled water with constant stirring at 80°C for 4 hours. The excess solvent was removed by evaporation with continuous stirring; the resultant precursor was dried at 110°C for 12 hours and then finally calcined at 500°C for 4 hours in high temperature muffle furnace under static air atmosphere.

The synthesis of Cr-doped TiO_2 nanoparticles was carried out by modified sol-gel method using water-alcohol mixture as a solvent, the only difference was that precursor solution was mixed with 100 ml distilled water containing variable concentrations (1, 3 and 5 mole %) of chromium nitrate nonahydrate under constant stirring at 80°C for 4 hours. The Resultant powders were labeled as x % CrT, where x % is the mole % Cr in TiO_2.

2.3. Characterization

The synthesized nanocrystalline powders were characterized by various sophisticated techniques such as X-ray diffraction (XRD) patterns were recorded on a model Philips X-ray diffractometer with diffraction angle 2θ in between 20 to 80° using Cu-Kα radiation of wavelength 1·54058 Å. Surface morphology and elemental analysis of the samples were carried out using scanning electron microscopy with electron dispersion spectroscopy (SEM-EDX) characterization was conducted using FEI Nova Nano SEM 450. UV-vis diffuse reflectance spectra (UV-vis-DRS) were recorded at room temperature in the wavelength range of 200-800 nm using Varian Carry 5000.

3. RESULTS AND DISCUSSION

After calcination at 500°C, the resultant nanocrystalline powders were analyzed to study their surface morphology and composition with help sophisticated analytical instrumental techniques. Photocatalytic potency was further tested for methyl red (MR) dye degradation.

3.1. X-Ray Diffraction

The XRD pattern of undoped and Cr-doped TiO_2 nanoparticles calcined at 500°C is shown in Fig.1. The XRD peaks of all the synthesized samples were wide confirming the nanocrystalline nature of the photocatalyst. The peak values located at 2θ(º) 25.2, 37.6, 48.0, 53.8, 54.9, 62.6, 68.7, 70.2 and 74.9 correspond to the Miller indices (101), (004), (200), (105), (210), (204), (214), (220) and (107) respectively, confirming formation of highly photoactive tetragonal anatase Titania. All the diffraction peaks obtained from XRD agreed with the reported JCPDS card no. 21-1272 for tetragonal anatase Titania. No distinct peaks corresponding to the rutile phase or dopant were see ninth X-ray diffractograms, which may be due to the proper incorporation of Cr^{3+}ions into the TiO_2 lattice. The crystallite sizes were estimated with the

help of Scherer's equation, by using the most intense reflection (2 θº = 25.4) and were found to be in the range of 5.9 to 18.8 nm

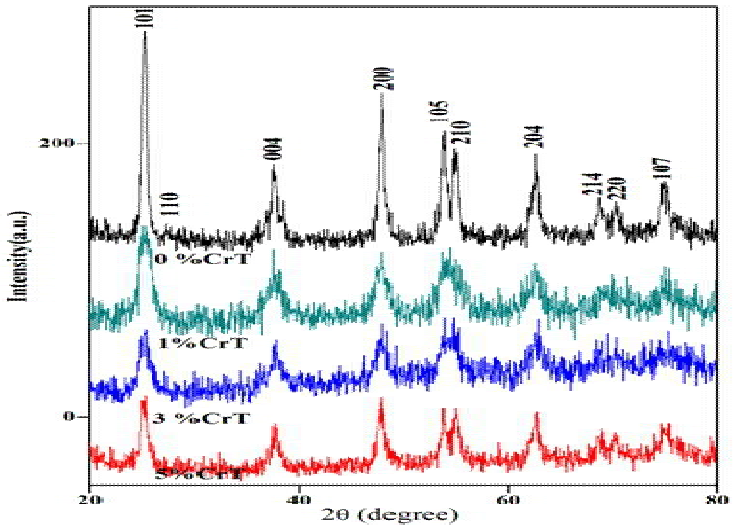

Fig. 1. XRD patterns of chromium doped and undoped titania.

Table 1. Physical parameters of Cr doped and undoped Titania nanoparticles obtained from X-Ray Diffraction and Diffuse Reflectance Spectroscopy.

Sr. No.	Catalyst	Crystallite size, (nm)	Bandgap energy, (eV)
1.	0% CrT	18.8	3.12
2.	1% CrT	7.0	2.7
3.	3% CrT	5.9	2.5
4.	5% CrT	6.6	2.4

3.2. Scanning electron microscopy (SEM) analysis

Fig. 2 (a, b) shows the SEM micrograph of 1mol% Cr (III)–doped TiO_2 photocatalyst. Both the images show particles with uniform distribution and spherical like morphology.

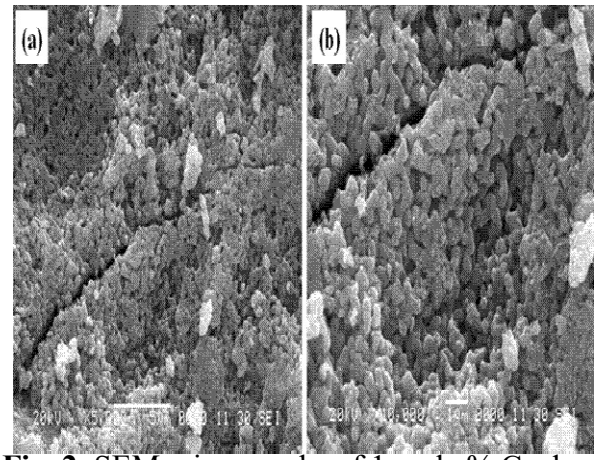

Fig. 2. SEM micrographs of 1 mole % Cr-doped Titania calcined at 500°C.

3.3. EDX analysis

The energy dispersive X-ray spectrum (EDXS) of 1 mol% Sm(III)-doped TiO_2 is shown in Fig. 3. It shows peaks corresponding to Ti, Sm, and O only. EDX result supports the doping of Sm in TiO_2.

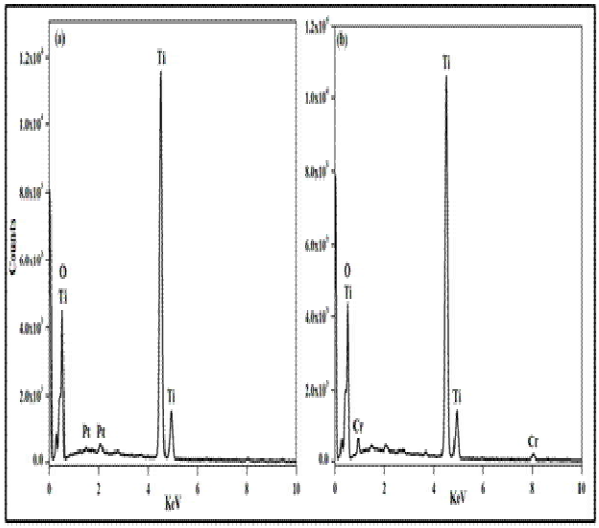

Fig. 3. EDX pattern for undoped and 1 mole% Cr-doped calcined at 500°C.

Table 2. Elementalanalysis synthesized nanomaterials by the EDX technique.

No.	Photocatalyst	Elements	Wt. %	Atomic	Mole %
1.	TiO_2	O	67.08	85.92	75.03
		Ti	32.92	14.08	24.37
2.	1% $CrTiO_2$	O	64.36	84.49	73.14
		Ti	34.52	15.14	26.22
		Cr	1.12	0.37	0.64
3.	3% $CrTiO_2$	O	66.54	85.79	75.10
		Ti	31.63	13.62	23.86
		Cr	1.82	0.59	1.03
4.	5% $CrTiO_2$	O	51.10	76.14	61.46
		Ti	44.99	22.39	36.17
		Cr	3.91	1.47	2.37

3.4. TEM analysis

The surface morphology of synthesized nanomaterial was studied by TEM analysis; figure 4 shows the TEM image of 1% Cr-TiO_2 nanomaterials calcined at 500°C. From TEM analysis, it is clear that the synthesized nanoparticles are denser and spherical in shape as shown in figure 4 (a-b) with excellent crystallinity seen in figure 4 (c). The SAED pattern confirms the presence of

the anatase phase as shown in figure 4 (a) which supported XRD analysis. The d-spacing was indexed with the JCPDS card No 21-1272 corresponding to the anatase phase. The grain sizes were calculated from TEM analysis and were found in the range between 8-10 nm; thus, results obtained from TEM are in good agreements with XRD analysis

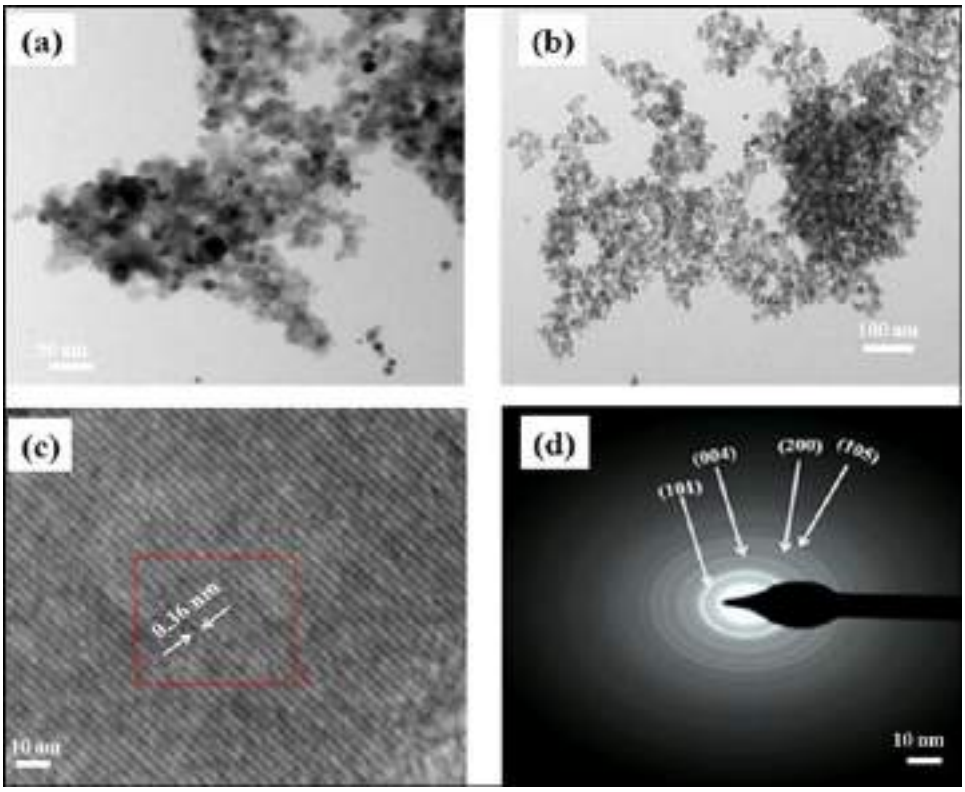

Fig. 4. Typical TEM and HRTEM micrographs of synthesized nanoparticles: (a, b) TEM images at different magnifications; (c) HR-TEM image and (d) SAED pattern of 1 mole % Cr^{3+} doped TiO_2 calcined at 500°C.

3.5. Ultra-Violet Visible Diffuse Reflectance Spectroscopy (UV-Vis DRS)

To study optical absorption properties, all the synthesized nanomaterials were analyzed by UV-Visible DRS technique in the absorption range of 200 nm to 700 nm and the results are shown in Fig.4. The bare Titania shows the absorption at 404 nm with bandgap energy 3.12 eV, which is near the bandgap energy of the anatase Titania (∽3.2 eV). While significant enhancement in the absorption edge was observed for all doped samples indicating a red shift in the absorption of wavelength in between 400–700 nm. The doping of transition metal ions like Cr^{3+} ions does no modify the position of valance band edge of Titania but it introduces new energy levels into the bandgap of Titania. Thus, the dopant energy levels in between valance band and conduction band shift the absorption edge towards longer wavelength resulting in the decrease of bandgap energy.

The bandgap energy values were calculated by extrapolation of the absorption band to the x-axis using the following equation,

$E_{bg} = 1240/\lambda$ ---Equation 1

Where, λ is the wavelength in nanometer and E_{bg} is the band gap energy. The calculated band gap energy values were, in the range of 2.5 to 3.1 eV (Table 1).

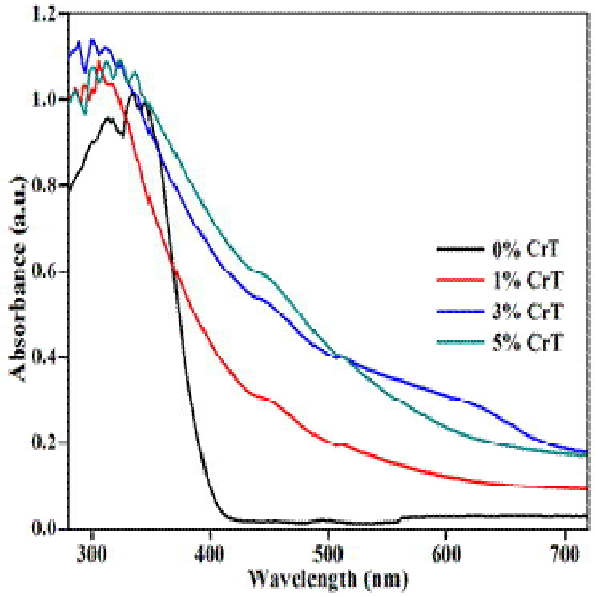

Fig. 5. UV-DR Spectra of doped and Cr(III)-doped TiO_2 nanoparticles calcined at 500°C.

3.6. Evaluation of Photocatalytic Activity of the Samples

The photocatalytic degradation was carried out with 200 ml (50 ppm) aqueous MR solution containing 50 mg of a catalyst under visible light irradiation using an artificial radiation source (tungsten filament lamp, 200 W). For better dispersion of catalyst powder, the resultant mixture was first ultra-sonicated for 10 minutes and then stirred in the dark for 30 minutes to reach adsorption equilibrium. Then, the mixture was placed inside the photoreactor in which the vessel was 6 - 7 cm away from the radiation source. These experiments were performed at room temperature. The small allocate of the mixture was taken at periodic intervals during the irradiation and after centrifugation; it was analyzed by UV-Vis spectrophotometer. The change in MR concentration was analyzed by a UV-vis spectrophotometer and the absorption peak at 525 nm was recorded. A gradual decrease in dye concentration was observed from the absorption spectra within 3 hours. Figure 6 compares the catalytic activity of all catalysts for MG degradation. It was found that all the doped samples show efficient photocatalytic activity towards dye degradation. The activity result also shows that among all catalysts, 3 mole% Cr^{3+}-doped TiO_2 shows the best activity than all other catalytic materials tested under similar experimental conditions. Among all doped samples 3 mole% chromium doped samples show the highest photocatalytic efficiency and near about 93 % dye degrades within 300 minutes of irradiation times with catalysts does 50 mg and at 50 ppm initial dye concentration. The activity

of all other catalysts follows the order given below; 3 % CrT >>5% CrT > 1% CrT> 0% CrT. All the doped nanomaterials show higher photocatalytic activity than other photocatalysts due to their small grain size, high crystallinity with the shift of absorption maxima towards the visible light region. The highest photocatalytic activity was recorded for 3 mole % chromium doped Titania, this is the maximum limits of dopant concentration, and above this concentration, a dopant may act as a recombination center for photogenerated charged particles (e^-/h^+). Due to the highly crystalline but smaller particle size, the photogenerated carriers diffuse fast to the surface and react rapidly with the adsorbed dye molecules and hence an effective utilization of charge carriers, especially holes for oxidation.

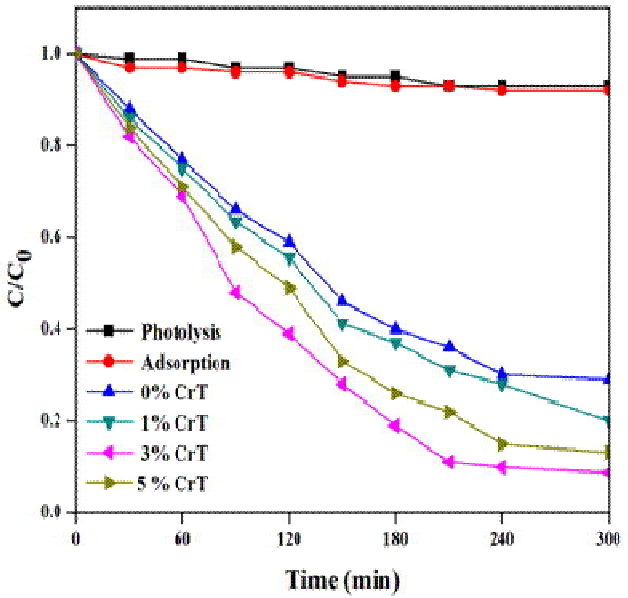

Fig. 7. Temporal evolution of MR removal during photocatalytic experiments under visible light irradiation.

4. CONCLUSION

Visible light-induced highly photocatalytic active of Cr(III)-doped TiO_2 nanoparticles have been successfully synthesized by the surfactant modified sol-gel method. The results from XRD, SEM–EDX, TEM-HR-TEM, and UV–Vis confirms the formation of anatase as a dominant crystalline phase, a decrease in the grain size and shifting of absorption maxima towards longer wavelength for all chromium doped photocatalyst. The photocatalytic activity results showed that all the chromium doped nanocrystalline materials show enhanced in the photodegradation efficiency for MR dye and it was also found that 3.0 mol% Cr(III)-TiO_2 shows highest photodegradation efficiency under the visible light irradiation. The small grain size and red shifts in the band-gap transition, higher e^-/h^+ pair separation efficiency of chromium doped samples favors the photocatalytic efficiency.

5. ACKNOWLEDGMENTS

The authors are grateful to the Principal, Shri Dnyaneshwar Mahavidyalaya, Newasa for providing the all required facilities to carry out the work.

6. REFERENCES

1. Akpan, U. G., & Hameed, B. H. (2009). Parameters affecting the photocatalytic degradation of dyes using TiO2-based photocatalysts: a review. *Journal of hazardous materials*, *170*(2-3), 520-529.
2. Dinkar, V. A., Shridhar, S. J., Madhukar, E. N., Anil, E. A., & Nitin, H. K. (2016). Sm-Doped Tio2 Nanoparticles with High Photocatalytic Activity for ARS Dye Under Visible Light Synthesized by Ultrasonic Assisted Sol-Gel Method. *Oriental Journal of Chemistry*, *32*(2), 933-940.
3. Chen, D., Sivakumar, M., & Ray, A. K. (2000). Heterogeneous photocatalysis in environmental remediation. *Developments in Chemical Engineering and Mineral Processing*, *8*(5-6), 505-550.
4. Chen, J. S., Tan, Y. L., Li, C. M., Cheah, Y. L., Luan, D., Madhavi, S., ... & Lou, X. W. (2010). Constructing hierarchical spheres from large ultrathin anatase TiO2 nanosheets with nearly 100% exposed (001) facets for fast reversible lithium storage. *Journal of the American Chemical Society*, *132*(17), 6124-6130.
5. Dholam, R., Patel, N., Adami, M., & Miotello, A. (2009). Hydrogen production by photocatalytic water-splitting using Cr-or Fe-doped TiO2 composite thin films photocatalyst. *International Journal of Hydrogen Energy*, *34*(13), 5337-5346.
6. Dodd, A. C., McKinley, A. J., Saunders, M., & Tsuzuki, T. (2006). Effect of particle size on the photocatalytic activity of nanoparticulate zinc oxide. *Journal of Nanoparticle Research*, *8*(1), 43.
7. Dvoranova, D., Brezova, V., Mazúr, M., & Malati, M. A. (2002). Investigations of metal-doped titanium dioxide photocatalysts. *Applied Catalysis B: Environmental*, *37*(2), 91-105.
8. Fujishima, A., Zhang, X., & Tryk, D. A. (2007). Heterogeneous photocatalysis: from water photolysis to applications in environmental cleanup. *International journal of hydrogen energy*, *32*(14), 2664-2672.
9. Hoffmann, M. R., Martin, S. T., Choi, W., & Bahnemann, D. W. (1995). Environmental applications of semiconductor photocatalysis. *Chemical Reviews*, *95*(1), 69-96.
10. Ihara, T., Miyoshi, M., Iriyama, Y., Matsumoto, O., & Sugihara, S. (2003). Visible-light-active titanium oxide photocatalyst realized by an oxygen-deficient structure and by nitrogen doping. *Applied Catalysis B: Environmental*, *42*(4), 403-409.
11. Jo, W. K., & Kim, J. T. (2009). Application of visible-light photocatalysis with nitrogen-doped or unmodified titanium dioxide for control of indoor-level volatile organic compounds. *Journal of Hazardous Materials*, *164*(1), 360-366.
12. Kim, S., Kim, M., Hwang, S. H., & Lim, S. K. (2012). Enhancement of photocatalytic activity of titania–titanate nanotubes by surface modification. *Applied Catalysis B: Environmental*, *123*, 391-397.
13. Kim, S., Kim, M., Kim, Y. K., Hwang, S. H., & Lim, S. K. (2014). Core–shell-structured carbon nanofiber-titanate nanotubes with enhanced photocatalytic activity. *Applied*

Catalysis B: Environmental, *148*, 170-176.

14. Kuriakose, S., Bhardwaj, N., Singh, J., Satpati, B., & Mohapatra, S. (2013). Structural, optical and photocatalytic properties of flower-like ZnO nanostructures prepared by a facile wet chemical method. *Beilstein journal of nanotechnology*, *4*(1), 763-770.

15. Colmenares, J. C., Aramendia, M. A., Marinas, A., Marinas, J. M., & Urbano, F. J. (2006). Synthesis, characterization and photocatalytic activity of different metal-doped titania systems. *Applied Catalysis A: General*, *306*, 120-127.

16. Bechstein, R., Kitta, M., Schütte, J., Onishi, H., & Kühnle, A. (2009). The effects of antimony doping on the surface structure of rutile TiO2 (110). *Nanotechnology*, *20*(26), 264003.

17. V. A., & Soofivand, F. (2014). RSC Advances. *RSC Adv*, *4*, 27654–27660.

18. Peng, Y. H., Huang, G. F., & Huang, W. Q. (2012). Visible-light absorption and photocatalytic activity of Cr-doped TiO2 nanocrystal films. *Advanced Powder Technology*, *23*(1), 8-12.

19. Rauf, M. A., Meetani, M. A., & Hisaindee, S. (2011). An overview on the photocatalytic degradation of azo dyes in the presence of TiO2 doped with selective transition metals. *Desalination*, *276*(1-3), 13-27.

20. Sánchez-Muñoz, S., Pérez-Quintanilla, D., & Gómez-Ruiz, S. (2013). Synthesis and photocatalytic applications of nano-sized zinc-doped mesoporous titanium oxide. *Materials Research Bulletin*, *48*(2), 250-255.

21. de Souza, M. L., & Corio, P. (2013). Effect of silver nanoparticles on TiO2-mediated photodegradation of Alizarin Red S. *Applied Catalysis B: Environmental*, *136*, 325-333.

22. Lee, H. U., Lee, S. C., Choi, S. H., Son, B., Lee, S. J., Kim, H. J., & Lee, J. (2013). Highly visible-light active nanoporous TiO2 photocatalysts for efficient solar photocatalytic applications. *Applied Catalysis B: Environmental*, *129*, 106-113.

23. Wang, C., Ao, Y., Wang, P., Hou, J., Qian, J., & Zhang, S. (2010). Preparation, characterization, photocatalytic properties of titania hollow sphere doped with cerium. *Journal of hazardous materials*, *178*(1-3), 517-521.

24. Wang, W., Serp, P., Kalck, P., & Faria, J. L. (2005). Photocatalytic degradation of phenol on MWNT and titania composite catalysts prepared by a modified sol-gel method. *Applied Catalysis B: Environmental*, *56*(4), 305-312.

25. Yadav, H. M., Kolekar, T. V, Barge, A. S., Thorat, N. D., Delekar, S. D., Kim, B. M., Kim, J. S. (2015). Enhanced visible-light photocatalytic activity of Cr^{3+} -doped anatase TiO_2 nanoparticles synthesized by the sol-gel method. *J Mater Sci: Mater Electron*, *27*(1), 526–534.

26. Zhang, J., Wu, Y., Xing, M., Leghari, S. A. K., & Sajjad, S. (2010). Development of modified N doped TiO_2 photocatalyst with metals, non-metals, and metal oxides. *Energy & Environmental Science*, *3*(6), 715-726.

27. Zhang, X., Song, J., Jiao, J., & Mei, X. (2010). Preparation and photocatalytic activity of cuprous oxides. *Solid-State Sciences*, *12*(7), 1215-1219.

28. Zhang, X., Song, J., Jiao, J., & Mei, X. (2010). Preparation and photocatalytic activity of cuprous oxides. *Solid-State Sciences*, *12*(7), 1215-1219.